

Ultra-low capacitance and high speed germanium photodetectors on silicon

Long Chen and Michal Lipson

School of Electrical and Computer Engineering, Cornell University, Ithaca, NY 14853

lc286@cornell.edu

Abstract: We demonstrate waveguide integrated germanium detectors with capacitance as small as 2.4 fF and directly recorded impulse response as fast as 8.8 ps. Based on such detectors and cascaded silicon microring resonators we also demonstrate a highly scalable wavelength division demultiplexing system that can potentially provide tera-bit/s (Tbps) bandwidth over a small area.

©2009 Optical Society of America

OCIS codes: (040.5160) Photodetectors; (250.5300) Photonic integrated circuits; (200.4650) Optical interconnects

References and links

1. D. A. B. Miller, "Rationale and challenges for optical interconnects to electronic chips," *Proc. IEEE* **88**, 728-749 (2000).
2. M. Haurylau, G. Chen, H. Chen, J. Zhang, N.A. Nelson, D. H. Albonese, E. G. Friedman, and P. M. Fauchet, "On-chip optical interconnect roadmap: challenges and critical directions," *IEEE J. Sel. Top. Quantum Electron.* **12**, 1699-1705 (2006).
3. H. Rong, A. Liu, R. Jones, O. Cohen, D. Hak, R. Nicolaescu, A. Fang, and M. Paniccia, "An all-silicon Raman laser," *Nature* **433**, 292-294 (2005).
4. A. Fang, H. Park, O. Cohen, R. Jones, M. Paniccia, and J. Bowers, "Electrically pumped hybrid AlGaInAs-silicon evanescent laser," *Opt. Express* **14**, 9203-9210 (2006).
5. A. Liu, R. Jones, L. Liao, D. Samara-Rubio, D. Rubin, O. Cohen, R. Nicolaescu, and M. Paniccia, "A high-speed silicon optical modulator based on a metal-oxide-semiconductor capacitor," *Nature* **427**, 615-618 (2004).
6. Q. Xu, B. Schmidt, S. Pradhan, and M. Lipson, "Micrometre-scale silicon electro-optic modulator," *Nature* **435**, 325-327 (2005).
7. W. M. J. Green, M. J. Rooks, L. Sekaric, and Y. A. Vlasov, "Ultra-compact, low RF power, 10 Gb/s silicon Mach-Zehnder modulator," *Opt. Express* **15**, 17106-17113 (2007).
8. Y. Vlasov, W. M. J. Green, and F. Xia, "High-throughput silicon nanophotonic wavelength-insensitive switch for on-chip optical networks," *Nature Photonics* **2**, 242 - 246 (2008).
9. N. Sherwood-Droz, H. Wang, L. Chen, B. G. Lee, A. Biberman, K. Bergman, and M. Lipson, "Optical 4x4 hitless silicon router for optical Networks-on-Chip (NoC)," *Opt. Express* **16**, 19395-19395 (2008).
10. H. Park, A. W. Fang, R. Jones, O. Cohen, O. Raday, M. Sysak, M. Paniccia, and J. Bowers, "A hybrid AlGaInAs-silicon evanescent waveguide photodetector," *Opt. Express* **15**, 6044-6052 (2007).
11. G. Dehlinger, S. J. Koester, J. D. Schaub, J. O. Chu, Q. C. Ouyang, and A. Grill, "High-speed Germanium-on-SOI lateral PIN photodiodes," *IEEE Photon. Technol. Lett.* **16**, 2547-2549 (2004).
12. D. Ahn, C. Hong, J. Liu, W. Giziewicz, M. Beals, L. C. Kimerling, J. Michel, J. Chen, and F. X. Kärtner, "High performance, waveguide integrated Ge photodetectors," *Opt. Express* **15**, 3916-3921 (2007).
13. L. Vivien, M. Rouvière, J. Fédéli, D. Marris-Morini, J. Damlencourt, J. Mangeney, P. Crozat, L. Melhaoui, E. Cassan, X. Roux, D. Pascal, and S. Laval, "High speed and high responsivity germanium photodetector integrated in a Silicon-On-Insulator microwaveguide," *Opt. Express* **15**, 9843-9848 (2007).
14. T. Yin, R. Cohen, M. Morse, G. Sarid, Y. Chetrit, D. Rubin, and M. J. Paniccia, "31GHz Ge n-i-p waveguide photodetectors on Silicon-on-Insulator substrate," *Opt. Express* **15**, 13965-13971 (2007).
15. L. Chen, P. Dong, and M. Lipson, "High performance germanium photodetectors integrated on submicron silicon waveguides by low temperature wafer bonding," *Opt. Express* **16**, 11513-11518 (2008).
16. L. Tang, S. E. Kocabas, S. Latif, A. K. Okyay, D. Ly-Gagnon, K. C. Saraswat, and D. A. B. Miller, "Nanometre-scale germanium photodetector enhanced by a near-infrared dipole antenna," *Nature Photon.* **2**,

226-229 (2008).

17. The drift velocity of electrons in germanium saturates at $\sim 6 \times 10^4$ m/s with electrical field of 5×10^5 V/m, and holes reach 90% of its saturated velocity of the same value at electrical field of 1×10^6 V/m. See Levinshtein, M. & Simin, G.S. *Getting to Know Semiconductors* (World Scientific, 1992).
18. Q. Tong, L. Huang, and U. Gosele, "Transfer of semiconductor and oxide films by wafer bonding and layer cutting," *J. of Electron. Materials* **29**, 928-932 (2000).
19. W.C. Dash and R. Newman, "Intrinsic optical absorption in single crystal germanium and silicon at 77°K and 300°K," *Phys. Rev.* **99**, 1151-1155 (1955).
20. M. Rouviere, M. Halbwx, J. L. Cercus, E. Cassan, L. Vivien, D. Pascal, M. Heitzmann, and J. M. Hartmann, "Integration of germanium waveguide photodetectors for intrachip optical interconnects," *Opt. Eng.* **44**, 75402-75406 (2005).
21. S. Y. Chou, W. Khalil, T. Y. Hsiang, and S. Alexandrou, "Ultrafast nanoscale metal-semiconductor-metal photodetectors on bulk and low-temperature grown GaAs," *Appl. Phys. Lett.* **61**, 819-821 (1992).
22. Q. Xu, B. Schmidt, J. Shakya, and M. Lipson, "Cascaded silicon micro-ring modulators for WDM optical interconnection," *Opt. Express* **14**, 9430-9435 (2006).
23. B. E. Little, S. T. Chu, W. Pan, and Y. Kokubun, "Microring resonator arrays for VLSI photonics," *IEEE Photon. Technol. Lett.* **12**, 323-325 (2000).
24. S. Xiao, M. H. Khan, H. Shen, and M. Qi, "A highly compact third-order silicon microring add-drop filter with a very large free spectral range, a flat passband and a low delay dispersion," *Opt. Express* **15**, 14765-14771 (2007).
25. Q. Xu, D. Fattal, and R. G. Beausoleil, "Silicon microring resonators with 1.5- μm radius," *Opt. Express* **16**, 4309-4315 (2008).
26. L. Vivien, J. Osmond, J. Fédéli, D. Marris-Morini, P. Crozat, J. Damlencourt, E. Cassan, Y. Lecunff, and S. Laval, "42 GHz p.i.n Germanium photodetector integrated in a silicon-on-insulator waveguide," *Opt. Express* **17**, 6252-6257 (2009).
27. S. Assefa, F. Xia, S.W. Bedell, Y. Zhang, T. Topuria, P. M. Rice, and Y. A. Vlasov, "CMOS-Integrated 40 GHz germanium waveguide photodetector for on-chip optical interconnects," *Optical Fiber Communication Conference (OFC), OMR4* (2009).

The tremendous growth in computer processing power due to microelectronics scaling requires a corresponding increase in communication bandwidth. Optical interconnects, particularly silicon-based integrated photonics, could overcome traditional limitations of electrical interconnects and enable this increase [1-2]. To achieve this goal, individual optical components such as lasers, modulators, switches, routers and detectors have been demonstrated [3-15]. For on-chip applications, detectors with very small capacitance and high speed are crucial for low power, large bandwidth systems. Here we report germanium detectors with capacitance as small as 2.4 fF and directly recorded impulse response as fast as 8.8 ps, which are to the best of our knowledge the fastest integrated germanium detectors with an ultra-low capacitance. Based on such detectors we also demonstrate a highly scalable wavelength division demultiplexing system that can potentially provide tera-bit/s (Tbps) bandwidth over a small area.

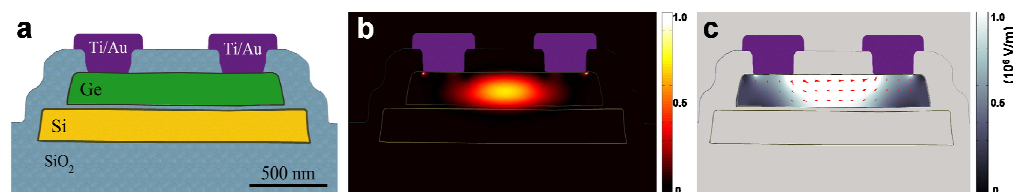


Fig. 1. Design of the waveguide integrated germanium MSM detector: (a) Cross-sectional schematic of the detector; (b) Optical energy distribution of its fundamental TE mode; (c) Strength (surface plot) and direction (cones) of the electrostatic field with 1V bias. The spatial overlap of optical mode in (b) and strong electrostatic field in (c) leads to very short transit time of the photo-generated carriers.

We use a waveguide integrated metal-semiconductor-metal MSM design optimized for small capacitance and fast response for transverse-electric (TE) polarization. Figure 1(a) shows a cross-sectional schematic of the device. Note that a thin layer of SiO₂ is introduced between germanium and silicon to prevent photo-generated carriers from diffusing into silicon that will degrade the speed. The parallel electrodes MSM configuration and the very thin germanium layer (260 nm) give rise to very low capacitance. Using finite-element electrostatic modeling, we calculated the capacitance for a 30 μm long detector to be 2.4 fF only, which is more than one order of magnitude lower than previously reported vertical PIN detectors [14]. This ultra-low capacitance allows a load resistance up to 1 kΩ for detector speed up to 60 GHz, which leads to a higher sensitivity and relaxed requirements on detector amplifiers and can reduce both optical and electrical power consumptions of the receiver [16]. The two planar electrodes also provide strong optical confinement and strong electrostatic field in the germanium region, ensuring efficient and fast collection of photo-generated carriers. Figure 1(b) shows the optical energy distribution for the fundamental TE mode. One can see that most of the light is confined between the two electrodes. Figure 1(c) shows the strength (color map) and directions (cones) of the electrostatic field in germanium with 1 V bias. The good spatial overlap of optical mode and electrostatic field leads to very short transit time of the photo-generated carriers. With an electrode spacing of 600 nm, the average transit time for both carriers can be as short as 7 ps [17], corresponding to a bandwidth over 60 GHz.

We fabricated the detectors with an ion-assisted layer cutting technique to obtain crystalline germanium on silicon and then standard CMOS processes to pattern the detectors and silicon waveguides [15,18]. With this approach, one can obtain high quality germanium films free of dislocation defects that are inherent to epitaxially grown germanium due to its large lattice mismatch with silicon [11-14]. We first prepared a standard 4-inch silicon-on-insulator wafer (from SOITEC, with 260 nm silicon and 3 μm buried oxide) covered with 80 nm SiO₂. For the germanium part we prepared a 4-inch germanium wafer (from Umicore, with resistivity > 40 Ω·cm) and implanted with H⁺ ions (dose 4×10¹⁶ cm⁻² at 80 KeV) for smart-cut. After surface clean, the two wafers were bonded at room temperature and then annealed at up to 400°C to initiate the layer splitting. The transferred germanium film was then chemical mechanical polished down to 260 nm. Electron beam lithography and reactive ion etching were then used repeatedly to define the germanium detectors, silicon waveguides, and detector vias, followed by evaporation and lift-off of the Ti/Au electrodes. The detectors are 30 μm long to ensure complete absorption of the light. The germanium cross-section is 1.5 μm x 0.26 μm, and the silicon region underneath the germanium is 1.8 μm x 0.26 μm. The planar electrodes are 0.35 μm wide with a spacing of 0.6 μm. Indeed the fabricated detectors show good performances in efficiency and dark current. The photocurrent completely saturates with bias voltage of 0.6 V, and shows less than 1% variation with higher voltage. Large quantum efficiency over 90% is estimated with wavelength below 1540 nm, which corresponds to the direct band gap of germanium [19,20]. At longer wavelengths the efficiency starts rolling-off as a result of the decreasing optical absorption coefficient. Note that no strong strain in the transferred germanium layer is expected since the direct wafer bonding between the germanium and SOI wafers was initiated at room temperature and subsequently annealed at fairly low temperature (100°C ~ 250°C) prior to layer splitting. Therefore the electronic band gap and optical absorption properties of the germanium film are expected to be close to those of crystalline bulk germanium substrate [19,20]. This is indeed confirmed with the experimentally measured spectral dependence of the detector responsivity [15]. The dark current of this particular device is about 4 μA at 5 V bias, which is one order of magnitude higher than our previous generation of device (~100 nA at 4 V, see [15]) due to accidental plasma damage of germanium surface during the via etch step before the electrode deposition.

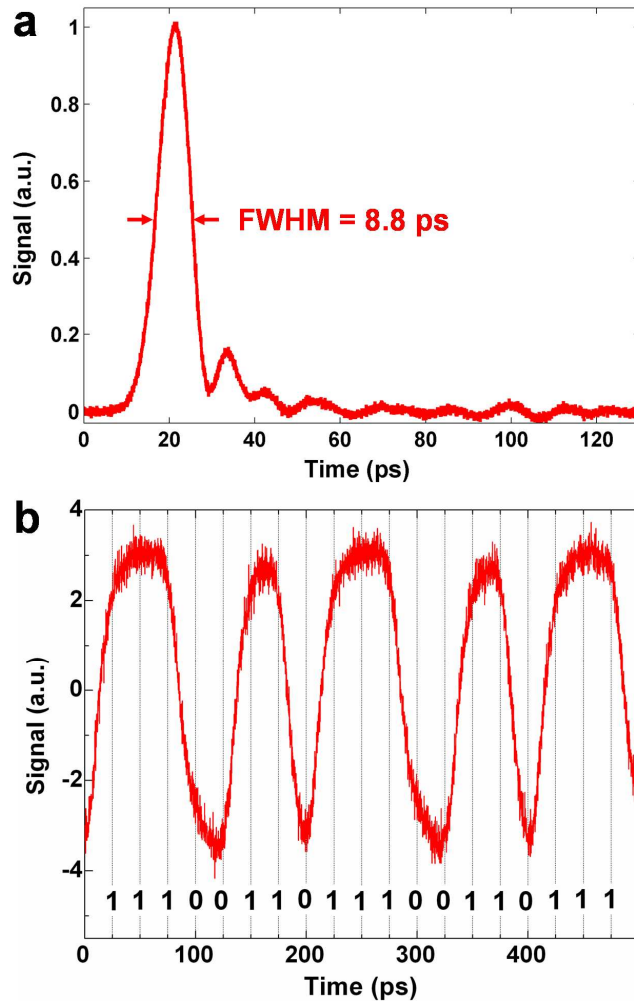


Fig. 2. (a) Detector temporal response to a ~ 1 ps pulse under a 5V bias (b) Detector response to an intensity modulated non-return-to-zero (NRZ) optical signal at 40 Gbps under a 4V bias.

We characterized the speed of the germanium detector by measuring its impulse response and demonstrated a pulse width as low as 8.8 ps. This was obtained by injecting a pico-second pulse from a fiber laser into a reference silicon waveguide terminated with a detector, and recording the temporal response of the photocurrent. The pulses are approximately 1 ps duration with 25 MHz repetition rate at 1550 nm. A fiber polarization controller was used to tune the input signal to TE polarization. A tapered tip at the end of the fiber and a nano-taper at the input end of the silicon waveguide were also used to increase the coupling efficiency to approximately -3 dB. A DC bias voltage was applied to the detector through a bias tee and RF probes, and the AC electrical responses were measured with a fast sampling oscilloscope. The measurement apparatus has a minimal bandwidth of 60 GHz. Due to the lack of transimpedance amplifier (TIA), the temporal response was averaged 25 times on the oscilloscope to reduce the sampler noise. Figure 2(a) shows the directly recorded temporal response under a 5 V bias. A full-width at half maximum (FWHM) of only 8.8 ps is observed here, which ideally corresponds to a bandwidth of about 50 GHz estimated from $f = 0.45/\tau_{FWHM}$ [21]. Note that no deconvolution is performed to factor out the response due to the measurement apparatus (for

example, the bias tee and sampler have quoted rise time of 3 ps and 3.4 ps, respectively), suggesting that the intrinsic response of the detector should be slightly faster than the value reported here. To the best of our knowledge this is the fastest integrated germanium detector reported with a very small capacitance, both of which are attributed to the optimized detector design as discussed earlier. The bandwidth estimated from Fourier transform of the impulse response is slightly lower (40 GHz) due to the small decay tail in Fig. 2(a). This tail originates from regions in the germanium with very weak electrostatic field (near the edges, see Fig. 1(c)), and can be eliminated by, for example, introducing high-level doping to form a horizontal PIN junction [11]. The primary pulse width is less than 10 ps with only 1 V bias, and the elimination of the tail will enable truly 50 GHz bandwidth with small bias voltage.

We also measured the detector response to an intensity modulated non-return-to-zero (NRZ) optical signal at 40 Gbps. The result for 4 V detector bias is plotted in Fig. 2(b). Despite some small pattern dependence between isolated “0” and consecutive “0”, clean detection of the digit pattern is observed here. The NRZ optical signals were generated by externally modulating a continuous wave laser with a LiNbO₃ optical intensity modulator. The electrical signal driving the modulator was obtained by time-multiplexing four signals at 10 Gbps data rate. The bias tee used for this particular measurement has a specified bandwidth of 50 GHz and a rise time of 7 ps. The temporal response in Fig. 2(b) was averaged five times using pattern lock feature of the oscilloscope to reduce the noise. Based on the results shown in Fig. 2(b) and the measured impulse response we believe data transmission at 40 Gbps data rate can be demonstrated with integrated amplifiers on the same silicon chip.

Based on these integrated detectors, we demonstrate a highly scalable wavelength division demultiplexing system with cascaded silicon microring resonators [22,23]. Figure 3(a) shows an optical microscope image of the device. A group of optical signals at various wavelength channels ($\lambda_1, \lambda_2, \dots, \lambda_N$) propagates along a silicon bus waveguide. Each of the microring resonators (see *Si demux* in Fig. 3(b)) is designed to resonate at one of these wavelengths (λ_i), and route only that channel from the bus waveguide to its drop port. Each dropped signal is then coupled to a broadband germanium photodetector. Note that the contact pads for probing are shared between neighboring detectors simply to reduce lithography time. Here as a proof of concept we demonstrate a 4-channel demultiplexer. The microring resonators are approximately 10 μm in radius with a cross-sectional dimension of 0.45 μm x 0.26 μm . The coupling gaps to the bus and drop waveguides (both are 400 nm wide) are 100 nm and 110 nm, respectively. The free spectra range (FSR) is calculated to be about 9 nm, and the channels are designed for a bandwidth of 0.16 nm (20 GHz) and a spacing of 1 nm (120 GHz).

We demonstrate a 4 x 19 GHz integrated detection system with the silicon demultiplexer and fast germanium detectors. Figure 3(c) shows DC spectra recorded with detectors at the end of the bus waveguide (through port) and the four drop-ports. Clean separation of the four wavelengths is observed here with a crosstalk between adjacent channels as low as -25 dB. Each channel has an optical bandwidth of approximately 0.15 nm (19 GHz) with a channel spacing of roughly 1 nm. The channel spacing between λ_1 and λ_2 is larger due to fabrication imperfection. The drop loss (the ratio of the dropped signal to the input signal) is -1 to -2 dB, which can be improved by reducing the propagation loss in the resonators and increasing the optical couplings to the bus and drop waveguides. To confirm the capability of demultiplexing optical data, we injected intensity-modulated optical signal centered at one of the channels into the bus waveguide and measured the response at corresponding drop-port detectors. Figure 3(d) shows an example of the recorded eye diagram for the 4th channel (1538.5 nm) at 15 Gbps. This data rate is limited only by the resonance bandwidth here. The slight closing of the eye observed here is due to signal distortion from the resonator due to the non-uniform transmission and dispersion within the passband.

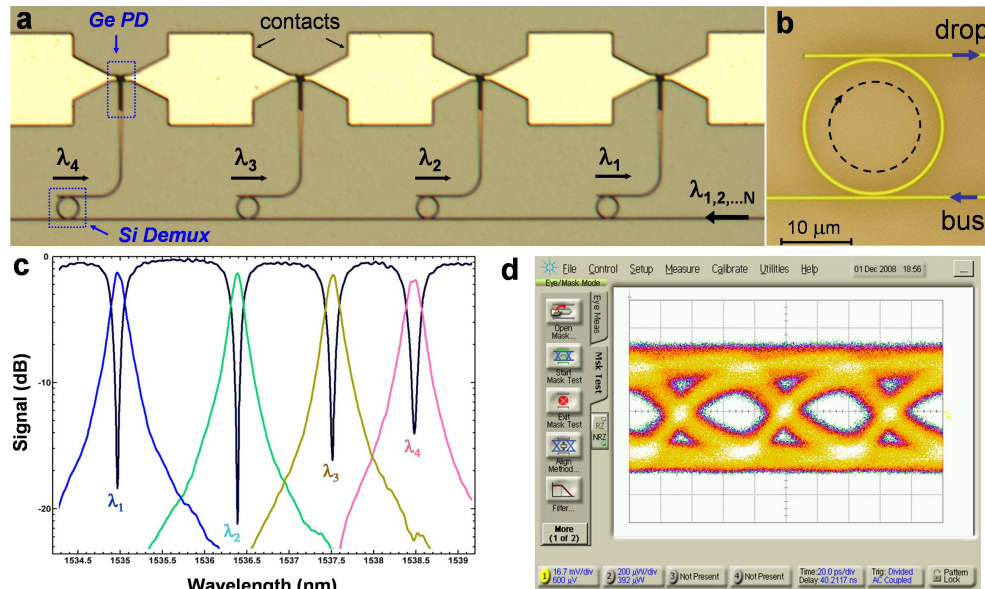


Fig. 3. Integrated detection system composed of silicon microring resonator-based wavelength division demultiplexer and the germanium detectors. (a) Optical image of the device; (b) Zoom-in of one microring resonator; (c) DC spectra of the through port and four drop ports measured with integrated detectors; (d) Eye diagram of demultiplexed data (λ_4) at 15 Gbps.

The demonstrated demultiplexer can be scaled to a bandwidth in the Tbps regime. Assuming 1 nm channel spacing, the resonance bandwidth can be broadened up to 0.4 nm (50 GHz – the detector bandwidth) while maintaining an estimated crosstalk level of -10 dB. Higher-order microring resonators can also be used to create flat passband and faster roll-off to reduce signal distortion and crosstalk [8,24]. Also, the maximum number of channels can be greatly enhanced with smaller resonator size and larger FSR. Microring resonators with more than 50 nm FSR can be obtained due to strong optical confinement of silicon waveguides [25], and therefore allow as many as 50 channels. Combining these optimized demultiplexers with our very fast, ultra-low capacitance detectors will ultimately lead to integrated receivers with 2.5 Tbps (50 x 50 Gbps) bandwidth, very low power consumption and a few mm² footprint.

Note added in revision: After the submission of our manuscript there are two publications reporting integrated germanium photodetectors with ~40 GHz bandwidth [26,27].

Acknowledgment

The authors would like to thank the National Science Foundation's CAREER Grant (No. 0446571) and its support through the Center for Nanoscale Systems (No. EEC-0117770). We also thank Christina Manolatu for the use of her finite difference mode solver. This work was performed in part at the Cornell Nano-Scale Science & Technology Facility (a member of the National Nanofabrication Users Network) which is supported by National Science Foundation, its users, Cornell University and Industrial Affiliates.